

ADVANCED ELECTROMAGNETIC ANALYSIS FOR ELECTRON SOURCE GEOMETRIES*

Mark Hess¹ and Chong Shik Park, IUCF, Bloomington, IN 47408, U.S.A.

Abstract

One of the challenging issues for analytically modeling electron sources, such as rf photoinjectors, is calculating time-dependent electromagnetic fields generated by the electron beam within a complicated conductor boundary. This problem can be handled self-consistently using a time-dependent Green's function method. We demonstrate this approach for a simplified electron source geometry, namely a semi-infinite circular pipe with a cathode. Following similar Lorentz gauge approaches that were used for computing electromagnetic potentials in low frequency (<1 GHz) photoinjectors [1,2], we present a compact Green's function solution for this simplified geometry. As an application, we show the electromagnetic potentials for a disk bunch of charge emanating from the cathode wall with acceleration parameters corresponding to the BNL 2.856 GHz 1.6 cell photocathode gun. [3]

INTRODUCTION

Currently, there are a number of analytical and numerical tools available for modeling electron source geometries, which include the effects of space-charge fields. In particular, the codes PARMELA [4], which incorporates electrostatic space-charge effects, and TREDI [5], which incorporates electromagnetic space-charge forces using Lienard-Wiechert potentials in free-space, have been extensively used for simulating photoinjectors. Recently, analytical techniques for computing electromagnetic potentials in low frequency (<1 GHz) photoinjectors have emerged in which bunch acceleration is assumed uniform and electromagnetic reflection from the cavity wall is negligible [1,2]. The electromagnetic potentials for the simplified source geometry, shown in Fig. 1, in the present paper were analyzed in Ref. 1 for the specific case of a uniform density bunch profile, which is uniformly accelerating in the longitudinal direction. Moreover, the integral form of the potentials in Ref. 1 require integration over rapidly oscillating terms in Fourier k -space.

In this paper, we start by following a similar Lorentz gauge formulation as in Ref. 1 for the geometry in Fig. 1, and present solutions to the electromagnetic potentials for arbitrary charge density and current density in the longitudinal direction which utilize a compact form for the Green's function in real space. This form requires integration over the sources in real space-time, but has the advantage of explicitly showing the causality conditions on real and image charges. This representation can be useful numerically when evaluating the potentials near the head of the bunch when causality effects are most important.

Our paper is organized as follows. In Sec. 2, the 3-D electromagnetic potentials are developed analytically for the cathode and circular pipe geometry. In Sec. 3, we use the potentials to numerically compute the electromagnetic fields for a disk-like bunch accelerating from rest off the cathode. In particular, the simulation parameters, including transverse beam size and longitudinal bunch motion, match the design parameters for the BNL 2.856 GHz 1.6 cell photocathode gun. [3] In Sec. 4, we give a summary of our results.

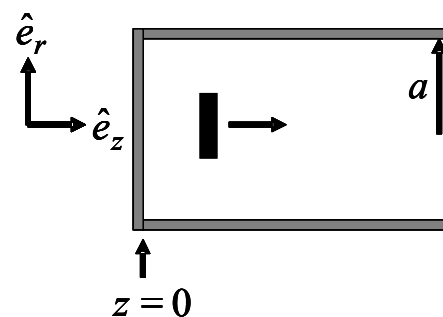


Figure 1: Schematic of system including conductor geometry and accelerating bunch.

ELECTROMAGNETIC POTENTIALS

A side profile of the conductor geometry under consideration, cathode and circular pipe, is shown in Fig. 1. The cathode location is designated by $z=0$ and the pipe is located at a radius of $r=a$. Also shown in Fig. 1 is a charged bunch moving in the longitudinal direction, whose charge density and current density are specified by $\rho(\vec{r}, t)$ and $J_z(\vec{r}, t)$, respectively. The non-zero electromagnetic potentials within the Lorentz gauge for the SI unit system are given by,

$$\left(\nabla^2 - \frac{1}{c^2} \frac{\partial^2}{\partial t^2} \right) \phi(\vec{r}, t) = -\frac{\rho(\vec{r}, t)}{\epsilon_0} \quad (1a)$$

$$\left(\nabla^2 - \frac{1}{c^2} \frac{\partial^2}{\partial t^2} \right) A_z(\vec{r}, t) = -\mu_0 J_z(\vec{r}, t). \quad (1b)$$

For self-consistency, the sources are assumed to satisfy the continuity equation

$$\frac{\partial \rho}{\partial t} + \frac{\partial J_z}{\partial z} = 0, \quad (2)$$

and the potentials satisfy the Lorentz gauge condition,

$$\frac{1}{c^2} \frac{\partial \phi}{\partial t} + \frac{\partial A_z}{\partial z} = 0. \quad (3)$$

The potentials also satisfy the appropriate boundary conditions at the pipe and cathode

*Work supported by Indiana University.

¹mhess@indiana.edu

$$\phi|_{r=a} = A_z|_{r=a} = 0 \quad (4a)$$

$$\left. \frac{\partial A_z}{\partial z} \right|_{z=0} = 0. \quad (4b)$$

The electromagnetic fields immediately follow from the potentials defined by Eqs. (1)-(4) using

$$\vec{E} = -\vec{\nabla}\phi - \partial\vec{A}/\partial t \quad (5a)$$

and

$$\vec{B} = \vec{\nabla} \times \vec{A}. \quad (5b)$$

The solutions to the potentials can be derived from two time-dependent Green's functions as

$$\phi(\vec{r}, t) = \frac{1}{\epsilon_0} \iint_{-\infty}^t G_\phi(\vec{r}, t; \vec{r}', t') \rho(\vec{r}', t') d^3\vec{r}' dt' \quad (6a)$$

and

$$A_z(\vec{r}, t) = \mu_0 \iint_{-\infty}^t G_A(\vec{r}, t; \vec{r}', t') J_z(\vec{r}', t') d^3\vec{r}' dt' \quad (6b)$$

where in the regime $z > 0$

$$\left(\nabla^2 - \frac{1}{c^2} \frac{\partial^2}{\partial t^2} \right) G_{\phi, A} = -\delta(\vec{r} - \vec{r}') \delta(t - t') \quad (7)$$

subject to the boundary conditions

$$G_\phi|_{r=a} = G_\phi|_{z=0} = 0 \quad (8a)$$

$$G_A|_{r=a} = \left. \frac{\partial G_A}{\partial z} \right|_{z=0} = 0. \quad (8b)$$

The solutions to the time-dependent Green's functions in Eqs. (7) and (8) are given by [6]

$$G_\phi = \frac{c}{2} \sum_{mn} \psi_{mn}(\vec{r}_\perp) \psi_{mn}^*(\vec{r}'_\perp) \times [J_0(k_{\perp mn} \lambda_-) \theta(\lambda_-^2) - J_0(k_{\perp mn} \lambda_+) \theta(\lambda_+^2)] \quad (9a)$$

$$G_A = \frac{c}{2} \sum_{mn} \psi_{mn}(\vec{r}_\perp) \psi_{mn}^*(\vec{r}'_\perp) \times [J_0(k_{\perp mn} \lambda_-) \theta(\lambda_-^2) + J_0(k_{\perp mn} \lambda_+) \theta(\lambda_+^2)], \quad (9b)$$

where

$$\psi_{mn}(\vec{r}_\perp) = \frac{1}{a\sqrt{\pi}} \frac{J_m(j_{mn} r/a) e^{im\theta}}{|J_{m+1}(j_{mn})|} \quad (10)$$

are the transverse eigenfunctions for the Helmholtz's equation in a circular pipe with Dirichlet boundary conditions,

$$k_{\perp mn} = j_{mn}/a \quad (11)$$

are the corresponding eigenvalues, $J_m(x)$ is the m th order Bessel function, j_{mn} is the n th positive root of $J_m(x)$, and

$$\lambda_\pm^2 = c^2(t - t')^2 - (z \pm z')^2. \quad (12)$$

We note that the gauge condition in Eq. (3) can be readily verified by using Eq. (2) along with integration by parts in Eq. (6). The factors $\theta(\lambda_-^2)$ and $\theta(\lambda_+^2)$ enforce the causality condition on the electromagnetic waves emanating from the bunch charge and induced image charges, respectively. When analyzing the potentials near the front of the bunch, these factors allow for rapid numerical convergence since only sources "sufficiently close" to the point of observation need to be considered.

DISK-BEAM SIMULATION

As an application of the electromagnetic equations derived in Sec. 2, we calculate potentials generated by a zero thickness disk bunch, which is created at the cathode at time $t=0$ and accelerated by an external rf electric field. We assume that the bunch charge density and current density are given by

$$\rho(\vec{r}, t) = \frac{3Q}{\pi r_b^2} \theta(r_b - r) \left(1 - \frac{r^2}{r_b^2} \right) \delta(z - z''(t)) \quad (13)$$

and

$$J_z(\vec{r}, t) = \frac{3Q}{\pi r_b^2} \frac{dz''}{dt} \theta(r_b - r) \left(1 - \frac{r^2}{r_b^2} \right) \delta(z - z''(t)), \quad (14)$$

where $z''(t)$ is the bunch trajectory specified by the following equations of motion for a charge in an rf-electric field,

$$dz''/dt = P_z/m_e \quad (15)$$

$$dP_z/dt = -eE_0 \cos(kz'') \sin(\omega t + \varphi). \quad (16)$$

In Eqs. (13) and (14), Q is the total bunch charge and r_b is the bunch radius. In Eqs. (15) and (16), P_z is the relativistic longitudinal momentum, m_e is the electron mass, e is the electron charge, E_0 is the maximum rf-electric field and $k = 2\pi f/c$, $\omega = 2\pi f$, and φ are the wavenumber, angular frequency, and injection phase of the rf-electric field.

As an example, we use the parameters for the BNL 1.6 cell photocathode gun [3], i.e. $f = 2.856$ GHz, $E_0 = 100$ MeV/m, $a = 4.111$ cm, $\varphi = 68^\circ$, $Q = 0.96$ nC, and $r_b = 1.0$ mm. Fig. 2 shows a plot of $z''(\tau)/\lambda$ (red) along with a light line (blue) versus $\tau = \omega t$, where $\lambda = c/f$ is the free-space wavelength of the injector.

Using the bunch trajectory in Fig. 2, we are able to compute $\phi(\vec{r}, t)$ and $A_z(\vec{r}, t)$ using Eqs. (6a) and (6b). In particular, we used $n \leq 500$ radial modes and numerical integration time-step of $d\tau = 0.001$ to compute the potentials. Figs 3(a), 3(b), 4(a), and 4(b) show plots of $\phi\omega\pi r_b^2 \epsilon_0/cQ$ and $A_z\pi r_b^2/\lambda cQ\mu_0$ for $\tau = 0.5$ and $\tau = 5.0$. We note that at $\tau = 0.5$ the bunch is located at $z''(\tau)/\lambda \cong 0.044$, and at $\tau = 5.0$, the bunch is located at $z''(\tau)/\lambda \cong 0.74$. We also note that the first waves from the

side wall reach the pipe axis at approximately $\tau = 5.0$. In a real photoinjector experiment, the first iris would be located at $z/\lambda = 0.25$ and the second iris $z/\lambda = 0.75$.

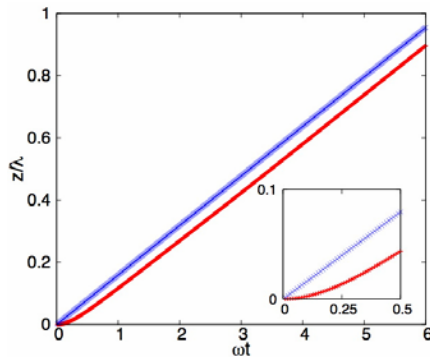


Figure 2: Plot of the bunch trajectory (red) and light line (blue) using the BNL 1.6 cell photocathode gun [1] parameters.

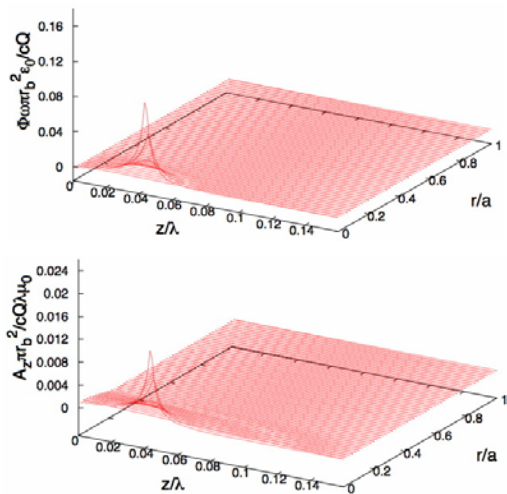


Figure 3: Plots of (a) normalized ϕ and (b) normalized A_z for $\tau = 0.5$.

SUMMARY

In summary, we have presented an analytical solution of the electromagnetic potentials inside of a cylindrical pipe with cathode using a compact Green's function method. The solutions for $\phi(\vec{r}, t)$ and $A_z(\vec{r}, t)$ in the Lorentz gauge were found within the framework of a time-dependent Green's function formulation, as was done in Ref. 1. However, unlike Ref. 1, our solutions are presented in real space rather than Fourier space for arbitrary charge and current density, and explicit show the causality conditions. This compact Green's function form allows for rapid numerical convergence of the electromagnetic potentials, in important regimes such as near the front of the bunch. We demonstrated the effectiveness of these potentials by simulating acceleration of a photoinjector bunch using the parameters for the BNL 2.856 GHz 1.6 cell photocathode gun. In the future, we are planning to incorporate the effects of disk-

like iris structures to form a more realistic model of the photoinjector.

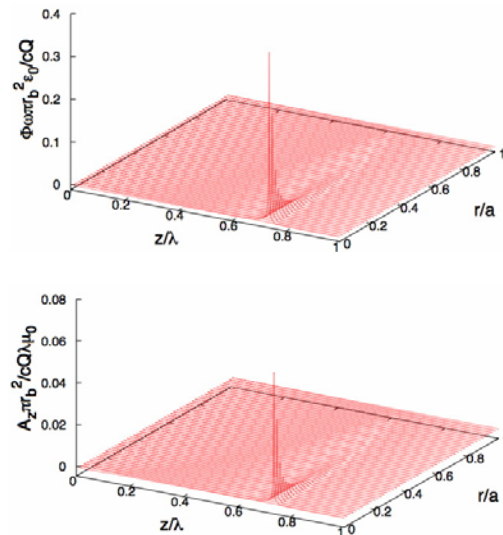


Figure 4: Plots of (a) normalized ϕ and (b) normalized A_z for $\tau = 5.0$.

ACKNOWLEDGEMENTS

The authors wish to thank the Indiana University Research SP supercomputing cluster for the usage of their computational facilities.

REFERENCES

- [1] W. Salah and J.M. Dolique, Nucl. Inst. and Meth A 447 (2004) 309.
- [2] W. Salah, Nucl. Inst. and Meth A 533 (2004) 248.
- [3] K. Batchelor et al, "Development of a High Brightness Electron Gun for the Accelerator Test Facility at Brookhaven National Laboratory", EPAC'88, Rome, June 1988.
- [4] L.M. Young (documentation by J.H. Billen), "PARMELA", report LA-UR-96-1835, Los Alamos, 1996 (rev. 2004).
- [5] L. Gianessi et al, Nucl. Inst. and Meth A 436 (1999) 443.
- [6] M. Hess and C. S. Park, to be submitted to PR-STAB (2005).